

**This is an electronic reprint of the original article.  
This reprint *may differ* from the original in pagination and typographic detail.**

**Author(s):** Turunen, Lotta; Peuronen, Anssi; Forsblom, Samu; Kalenius, Elina; Lahtinen, Manu;  
Rissanen, Kari

**Title:** Tetrameric and Dimeric [N⋯I+⋯N] Halogen-Bonded Supramolecular Cages

**Year:** 2017

**Version:**

**Please cite the original version:**

Turunen, L., Peuronen, A., Forsblom, S., Kalenius, E., Lahtinen, M., & Rissanen, K.  
(2017). Tetrameric and Dimeric [N⋯I+⋯N] Halogen-Bonded Supramolecular Cages.  
Chemistry: A European Journal, 23(48), 11714-11718.  
<https://doi.org/10.1002/chem.201702655>

All material supplied via JYX is protected by copyright and other intellectual property rights, and duplication or sale of all or part of any of the repository collections is not permitted, except that material may be duplicated by you for your research use or educational purposes in electronic or print form. You must obtain permission for any other use. Electronic or print copies may not be offered, whether for sale or otherwise to anyone who is not an authorised user.

# CHEMISTRY

## A European Journal

A Journal of



### Accepted Article

**Title:** Tetrameric and Dimeric [N•••I+•••N] Halogen-Bonded Supramolecular Cages

**Authors:** Kari Rissanen, Lotta Turunen, Anssi Peuronen, Samu Forsblom, Elina Kalenius, and Manu Lahtinen

This manuscript has been accepted after peer review and appears as an Accepted Article online prior to editing, proofing, and formal publication of the final Version of Record (VoR). This work is currently citable by using the Digital Object Identifier (DOI) given below. The VoR will be published online in Early View as soon as possible and may be different to this Accepted Article as a result of editing. Readers should obtain the VoR from the journal website shown below when it is published to ensure accuracy of information. The authors are responsible for the content of this Accepted Article.

**To be cited as:** *Chem. Eur. J.* 10.1002/chem.201702655

**Link to VoR:** <http://dx.doi.org/10.1002/chem.201702655>

Supported by  
**ACES**

WILEY-VCH

# Tetrameric and Dimeric [N⋯I<sup>+</sup>⋯N] Halogen-Bonded Supramolecular Cages

Lotta Turunen,<sup>[a]</sup> Anssi Peuronen,<sup>[a]</sup> Samu Forsblom,<sup>[a]</sup> Elina Kalenius,<sup>[a]</sup> Manu Lahtinen<sup>\*[a]</sup> and Kari Rissanen<sup>\*[a]</sup>

**Abstract:** Tripodal *N*-donor ligands are used to form halogen-bonded assemblies *via* structurally analogous Ag<sup>+</sup>-complexes. Selective formation of discrete tetrameric I<sub>6</sub>L<sub>4</sub> and dimeric I<sub>3</sub>L<sub>2</sub> halonium cages, wherein multiple [N⋯I<sup>+</sup>⋯N] halogen bonds are used in concert, can be achieved by using sterically rigidified cationic tris(1-methyl-1-azonia-4-azabicyclo[2.2.2]octane)-mesitylene ligand, **L1**(PF<sub>6</sub>)<sub>3</sub>, and flexible ligand 1,3,5-tris(imidazole-1-ylmethyl)-2,4,6-trimethylbenzene, **L2**, respectively. The iodonium cages, I<sub>6</sub>L<sub>4</sub>(PF<sub>6</sub>)<sub>18</sub> and I<sub>3</sub>L<sub>2</sub>(PF<sub>6</sub>)<sub>3</sub>, were obtained through the [N⋯Ag<sup>+</sup>⋯N] → [N⋯I<sup>+</sup>⋯N] cation exchange reaction between the corresponding Ag<sub>6</sub>L<sub>4</sub>(PF<sub>6</sub>)<sub>18</sub> and Ag<sub>3</sub>L<sub>2</sub>(PF<sub>6</sub>)<sub>3</sub> coordination cages, prepared as intermediates, and I<sub>2</sub>. The synthesized metallo- and halonium cages were studied in solution by NMR, in gas phase by ESI-MS and in the solid-state by single crystal X-ray diffraction.

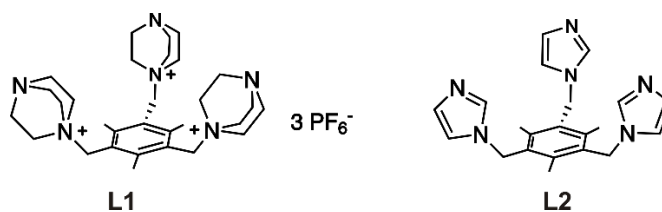
## Introduction

Halogen bonding (XB) is a non-covalent interaction between a polarized halogen atom and a Lewis base.<sup>[1]</sup> During the last decade XB has found applications in variety of research fields including crystal engineering, material sciences, medicinal chemistry and organocatalysis.<sup>[2]</sup> Halonium ions are interesting class of XB donors which are able to form three-center-four-electron (3c4e) bonds with two XB acceptor moieties.<sup>[3,4]</sup> Behavior of halonium ions in bis-pyridine complexes have been carefully studied in solution and in the solid-state.<sup>[3,5–7]</sup> Recently, we reported syntheses and characterizations of dimeric and hexameric capsules solely based on [N⋯I<sup>+</sup>⋯N] bonds.<sup>[8]</sup> It has been shown that [N⋯I<sup>+</sup>⋯N] bond is a strong interaction that exhibits highly predictable bond parameters.<sup>[4]</sup> Hence, it is particularly well-suited for the self-assembly studies of halogen-bonded supramolecular species/complexes.

Among different supramolecular assemblies coordination cages, as metallosupramolecular complexes, have attracted particular attention during the last two decades. The keen interest toward coordination cages is partly due to their fascinating structural features, but also because of the increase in number of potential applications that exploit their well-defined cavities.<sup>[9–13]</sup> These systems are prepared by coordination-driven

self-assembly from spatially pre-organized organic ligands (L) and metal cations (M) with known coordination geometry. One of the commonly used group of ligands is bowl-shaped tripodal *N*-donor ligands which enables the construction of various types of coordination cages such as dimeric M<sub>3</sub>L<sub>2</sub>, tetrahedral M<sub>6</sub>L<sub>4</sub> and octahedral M<sub>6</sub>L<sub>8</sub> species.<sup>[14,15]</sup> The exact cage topology is mostly governed by the connectivity and coordination geometry of the metal ion as well as the structural and chemical properties of the ligand. Furthermore, counter anions, reaction conditions (*e.g.* solvent and temperature) as well as possible auxiliary ligands can all have an effect to the outcome in the self-assembly process.

We have been interested in investigating the behavior of the [N⋯I<sup>+</sup>⋯N] halogen bond in connection with spatially organized multitopic XB acceptors.<sup>8</sup> In this work we extend this approach to two different tripodal XB acceptor ligands, **L1**(PF<sub>6</sub>)<sub>3</sub> and **L2** (Scheme 1), both of which have previously been used in the construction of coordination cages and are easily prepared according to the reported procedures.<sup>[16,17]</sup> The ligand **L2** is known to adapt different geometries due to the flexibility of the imidazole arms and hence different topologies including cages and polymeric structures with different metals and counter ions have been reported.<sup>[18–21]</sup> On the other hand, the self-assembly of **L1**(PF<sub>6</sub>)<sub>3</sub> with metal cations is to a great extent affected by the intra- and intermolecular steric interactions of the bulky DABCO groups which stabilize the bowl-shaped all-*cis* conformation of the ligand and restrict the spatial orientation of the *N*-donor moieties. Recently, we reported Pd<sup>2+</sup> and Cu<sup>2+</sup> based cages of **L1**<sup>3+</sup>.<sup>[22]</sup> Their self-assembly was shown to result in tetrahedral M<sub>6</sub>L<sub>4</sub> species instead of the expected M<sub>6</sub>L<sub>8</sub> due to the steric interactions between the DABCO groups around the metal node leading to linear N–M–N coordination. The corresponding Ag<sub>6</sub>L<sub>4</sub>(PF<sub>6</sub>)<sub>18</sub> was not known, but due to the linear nature of the [N⋯Ag<sup>+</sup>⋯N] bond, it was anticipated that once Ag<sub>6</sub>L<sub>4</sub>(PF<sub>6</sub>)<sub>18</sub> is obtained the [N⋯Ag<sup>+</sup>⋯N] → [N⋯I<sup>+</sup>⋯N] cation exchange reaction would result in the analogous halogen-bonded tetrameric halonium cage I<sub>6</sub>L<sub>4</sub>(PF<sub>6</sub>)<sub>18</sub>.



**Scheme 1.** Structures of ligands **L1**(PF<sub>6</sub>)<sub>3</sub> and **L2**.

[a] M.Sc. L. Turunen, Dr. A. Peuronen, M.Sc. S. Forsblom, Dr. E. Kalenius, Dr. M. Lahtinen, Acad. Prof. K. Rissanen  
Department of Chemistry, NanoScience Center  
University of Jyväskylä  
P.O. Box 35, FI-40014 Jyväskylä (Finland)  
E-mail: kari.t.rissanen@jyu.fi

Supporting information for this article is given via a link at the end of the document.

In this contribution we report the results of NMR spectroscopic, mass spectrometric and single crystal X-ray structural studies of the  $[N\cdots I^+\cdots N]$  halogen-bonded tetrameric  $I_6L_4(PF_6)_{18}$  and dimeric  $I_3L_2(PF_6)_3$  halonium cages. Through the parent  $Ag^+$ -coordination complexes and, subsequently applying the  $[N\cdots Ag^+\cdots N] \rightarrow [N\cdots I^+\cdots N]$  cation exchange reaction,<sup>8</sup> we obtain the isostructural halogen-bonded cages. The single crystals of the halonium ion assemblies have turned out to be very challenging to obtain,<sup>8</sup> yet in this work we present the first X-ray structural characterization of the supramolecular cages constructed via multiple  $[N\cdots I^+\cdots N]$  halogen bonds.

## Results and Discussion

Syntheses of the  $[N\cdots I^+\cdots N]$  bonded capsules follow the previously reported procedures.<sup>8</sup> The halonium cages are obtained first by reacting  $L_1(PF_6)_3$  and  $L_2$  with silver hexafluorophosphate ( $AgPF_6$ ) followed by the addition of molecular iodine. The self-assembly of  $Ag^+$  and  $I^+$  species was monitored by  $^1H$  NMR in  $CD_3CN$  (Figure S1). Somewhat surprisingly, the addition of  $AgPF_6$  into the  $L_1(PF_6)_3$  in  $CD_3CN$  solution did not result in noticeable shifting of the  $L_1(PF_6)_3$  proton signals. This may be due to solvation of  $Ag^+$  as a  $[Ag(acetonitrile)_4]^+$  complex which seems to be energetically favored over the  $[Ag_6L_4]^{18+}$  in acetonitrile. However, after the addition of  $I_2$ , which was accompanied by an immediate precipitation of  $AgI$  and color change of the initially colorless solution to yellow (to mark the presence of slight excess of  $I_2$ ), the  $^1H$  NMR spectrum reveals a new set of downfield shifted  $L_1(PF_6)_3$  signals together with minor peaks of unreacted  $L_1(PF_6)_3$  (Figure S1c). Specifically, the merging of the two triplets that arise from the asymmetric DABCO environment into one peak at 3.6 ppm is due to the formation of the six symmetric  $[N\cdots I^+\cdots N]$  halogen bonds.

To provide more evidence for the expected formation of the  $[I_6L_4]^{18+}$  cage, diffusion-ordered NMR spectroscopy (DOSY) measurements were performed. Two set of signals were observed in the  $^1H$  DOSY spectrum of the expected  $I_6L_4(PF_6)_{18}$  indicating the presence of two discrete species (Figure S2). These were with diffusion coefficient ( $D$ ) of  $1.06 \times 10^{-9} m^2 \cdot s^{-1}$  and considerable lower value of  $6.09 \times 10^{-10} m^2 \cdot s^{-1}$  ( $CD_3CN$ , 298 K), which correspond to a mixture of unreacted  $L_1(PF_6)_3$  and a definitely larger species with radius of 1.05 nm (diameter of 2.1 nm) according to the Stokes-Einstein equation. The size correlates very well to our previous observations of  $Cu^{2+}$  and  $Pd^{2+}$  complexes with  $M_6L_4$  stoichiometry (size derived from the single crystal X-ray structure of  $Cu_6L_4(PF_6)_{24}$ ).<sup>[22]</sup>

Unfortunately, our efforts to characterize either  $Ag_6L_4(PF_6)_{18}$  or  $I_6L_4(PF_6)_{18}$  further with ESI-MS were not successful. This is not surprising considering the high positive charge density (+18) of the assemblies. In gas phase, the stabilizing solvent and anion interactions are absent and close proximity of the silver and iodonium cations with the cationic ligand likely results in repulsion and fragmentation of the cages.

The penultimate way to investigate the nature of the formed species is to crystallize both  $Ag_6L_4(PF_6)_{18}$  and  $I_6L_4(PF_6)_{18}$ .

Crystals emerged from a methanol solution of  $AgPF_6$  and  $L_1(PF_6)_3$  upon slow diffusion with ethyl acetate. Although no complexation between  $Ag^+$  and  $L_1(PF_6)_3$  was observed in solution by NMR, the single crystal X-ray analysis revealed the formation of a  $Ag_6L_4(PF_6)_{18}$  as a 2 nm cage (measured from the far-cornered H-atoms, Figure 1). The metallocage crystallized in a high-symmetry space group (tetragonal  $I-42m$ ) and is similarly two-fold disordered as the  $Cu_6L_4(PF_6)_{24}$  tetrameric cage.<sup>[22]</sup> The six  $Ag(I)$  ions and four ligands form a total of six  $[N\cdots Ag^+\cdots N]$  coordination environments with normal Ag-N bond distances and nearly linear to slightly bent N- $Ag^+$ -N bond angles, thus being structurally analogous to the  $Cu_6L_4(PF_6)_{24}$ .<sup>[22]</sup>

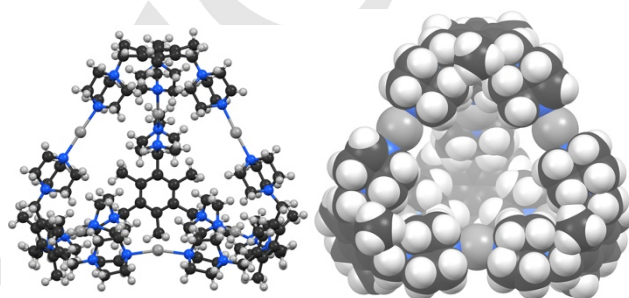


**Figure 1.** The ball-and-stick (left) and CPK (right) presentations of the crystal structure of  $Ag_6L_4(PF_6)_{18}$ . The N- $Ag$ -N bond lengths and angles are in the range of 2.27 - 2.32 Å and 160 - 177°, respectively. Disordered ligands, solvent molecules and all anions are omitted for clarity.

The reaction between  $Ag_6L_4(PF_6)_{18}$  and  $I_2$  in acetonitrile and the subsequent slow evaporation of the solvent led to the crystallization of colorless plates. The single crystal X-ray analysis of the crystals provided proof of the formation of the expected  $I_6L_4(PF_6)_{18}$  halonium cage (Figure 2). The solid state structure of  $I_6L_4(PF_6)_{18}$  consists of six  $I^+$  cations each of which binds to two distinct ligands resulting in a tetrahedral cage analogous to  $Ag_6L_4(PF_6)_{18}$  and  $Cu_6L_4(PF_6)_{24}$ .<sup>[22]</sup> Contrary to  $Ag_6L_4(PF_6)_{18}$ , the  $I_6L_4(PF_6)_{18}$  crystallizes in a lower symmetry space group (orthorhombic  $Pmna$ ) and does not show the symmetry-related two-fold disorder of the cage framework, thus facilitating its structural analysis. The six  $[N\cdots I^+\cdots N]$  halogen bonds have N-I distances ranging from 2.26 to 2.35 Å. The  $[N\cdots I^+\cdots N]$  halogen bonds are less symmetric than what is generally observed for  $[N\cdots I^+\cdots N]$  halogen bond from smaller XB acceptor moieties.<sup>[4]</sup> However, these have very seldom more than one undisturbed  $[N\cdots I^+\cdots N]$  halogen bond, whereas in  $I_6L_4(PF_6)_{18}$  the large and highly charged  $L_1$  ligand can induce geometric strains and distort each of the six  $[N\cdots I^+\cdots N]$  bonds. Nevertheless, only very minor bending from the ideally linear  $[N\cdots I^+\cdots N]$  halogen bonds occurs as all  $[N\cdots I^+\cdots N]$  angles are larger than 175°. This is characteristic to the  $[N\cdots I^+\cdots N]$  halogen bond, owing to the anisotropic charge distribution of the  $I^+$  cation, and is in stark contrast to the N- $Ag$ -N environments which are prone to higher coordination numbers and significant distortions from the linear coordination geometry. This highlights the predictable nature of the  $[N\cdots I^+\cdots N]$  halogen bond and its applicability in self-assembly of even larger supramolecular

assemblies.<sup>[8]</sup> Despite coordinative differences, the  $I_6L1_4(PF_6)_{18}$  binds the  $PF_6^-$  anions similarly as its metallosupramolecular analogues  $Ag_6L1_4(PF_6)_{18}$  and  $Cu_6L1_4(PF_6)_{24}$ <sup>[22]</sup>. Four out of the 18  $PF_6^-$  anions reside inside the endohedral cavity of the halonium cage, each occupying one of the four cationic ligand pockets. This anion binding arises primarily from the electrostatic interactions between the cationic  $L1^{3+}$  ligand and the anions.

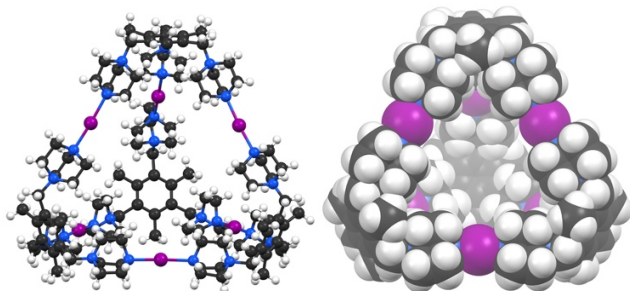


**Figure 2.** The ball-and-stick (left) and CPK (right) presentations of the crystal structure of  $I_6L1_4(PF_6)_{18}$ . The N–I–N bond lengths and angles are in the range of 2.26 - 2.35 Å and 175 - 177°, respectively. Solvent molecules and all anions are omitted for clarity.

As a structurally similar tripodal supramolecular building block **L2** has two significant differences to **L1**. Firstly, **L2** is non-charged and secondly has greater structural flexibility, meaning that by using different metal cations, counteranions, reaction conditions and metal-ligand stoichiometry, cages and polymeric structures are plausible.<sup>[18–21]</sup> Of these the  $I_3L2_2X_3$  is expected to be prominent as several  $Ag_3L2_2X_3$  complexes (where  $X = N_3^-$ ,  $NO_3^-$ ,  $ClO_4^-$ ,  $BF_4^-$ ,  $OTf^-$  or  $PF_6^-$ ) have been observed under similar conditions.<sup>[19,21,23,24]</sup> Contrary to highly-charged **L1**, **L2** does not impose additional electrostatic interactions and can lead to less-disturbed stronger  $[N \cdots I^+ \cdots N]$  halogen bonds.

The consecutive reactions of  $AgPF_6$  and  $I_2$  with **L2** in  $CD_3CN$  showed a shifted set of signals in  $^1H$  NMR spectrum in both cases. Comparison between the two spectra shows that  $I^+$  induces a larger downfield shift to the ligand signals than  $Ag^+$  (Figure 3). The  $^1H$  DOSY measurements (Figures 3d and S3) revealed single species for both  $Ag^+$  and  $I^+$  complexes with  $D$  of  $8.46 \times 10^{-10} \text{ m}^2 \cdot \text{s}^{-1}$  and  $7.86 \times 10^{-10} \text{ m}^2 \cdot \text{s}^{-1}$  in acetonitrile at 298K, respectively. The measured  $D$  values correspond to spherical objects with diameters of 1.52 nm and 1.63 nm whereas the corresponding estimated<sup>[18,19,21,23,24]</sup> values for  $M_3L2_2^{3+}$  and  $M_6L2_4^{6+}$  are roughly 1.3 - 1.4 nm and 1.65 - 1.9 nm, respectively. Hence, no conclusive analysis on the compositions can be drawn from the DOSY data alone. Instead, the composition was verified by ESI-MS analysis, in which only the formation of dimeric complex was detected and ions  $[I_3L2_2]^{3+}$  at  $m/z$  367 and  $[I_3L2_2+PF_6]^{2+}$  at  $m/z$  623 appeared in spectra (Figure S4 and Table S1). The possible tetrameric ions  $[I_6L2_4]^{6+}$  and  $[I_6L2_4+2PF_6]^{4+}$  could result in from overlapping  $m/z$  values of 367 and 623, but isotopic distributions and charge states corresponded only with the stoichiometry of the dimer.

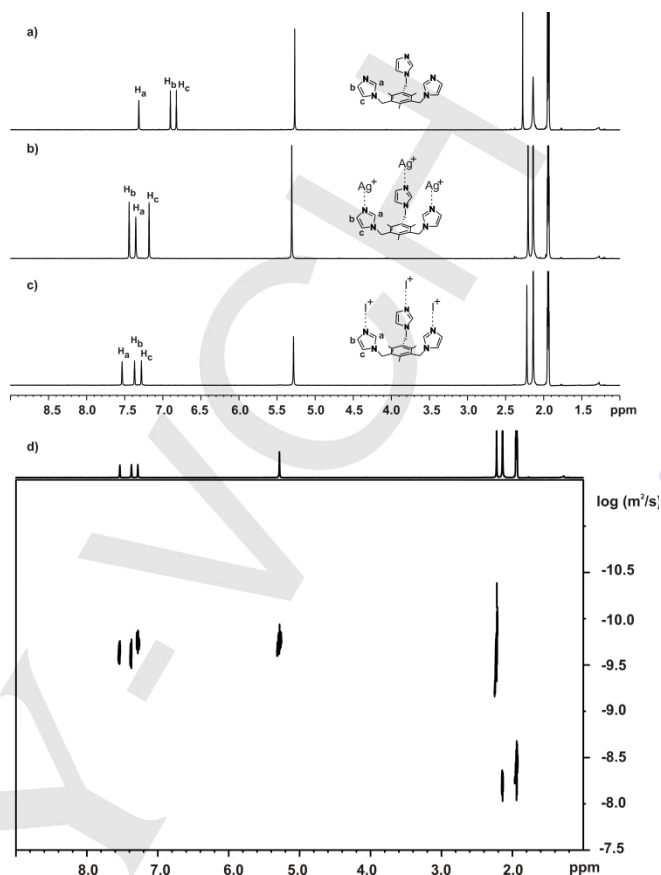


**Figure 3.**  $^1H$  NMR spectra ( $CD_3CN$ , 400 MHz, 298 K) of (a) **L2**, (b)  $Ag_3L2_2(PF_6)_3$  and (c)  $I_3L2_2(PF_6)_3$ , and (d) the  $^1H$  DOSY NMR spectrum of  $I_3L2_2(PF_6)_3$ .

The single crystals of  $Ag_3L2_2(PF_6)_3$  could be obtained by diffusing ethyl acetate into the respective acetonitrile solution whereas crystals of  $I_3L2_2(PF_6)_3$  emerged upon slow evaporation of an acetonitrile solution of  $Ag_3L2_2(PF_6)_3$  after reaction with  $I_2$  and filtration. The single crystal X-ray analysis confirmed the formation of the dimeric metallo- and halonium cages. The  $[N \cdots I^+ \cdots N]$  halogen bonds in the structure of  $I_3L2_2(PF_6)_3$  are symmetric and very close to linear with all six N–I distances and three N–I–N angles being 2.233(6) Å and 177.0(4)°, respectively due to the hexagonal crystal symmetry. Comparison of these bond parameters to the data available in the Cambridge Structural Database (CSD) shows that the  $[N \cdots I^+ \cdots N]$  halogen bonds in the  $I_3L2_2(PF_6)_3$  dimer are very close to the corresponding values of previously reported  $[N \cdots I^+ \cdots N]$  structures<sup>[25]</sup>, thus again nicely demonstrating the robustness and predictability of the  $[N \cdots I^+ \cdots N]$  halogen bond as a robust supramolecular motif.

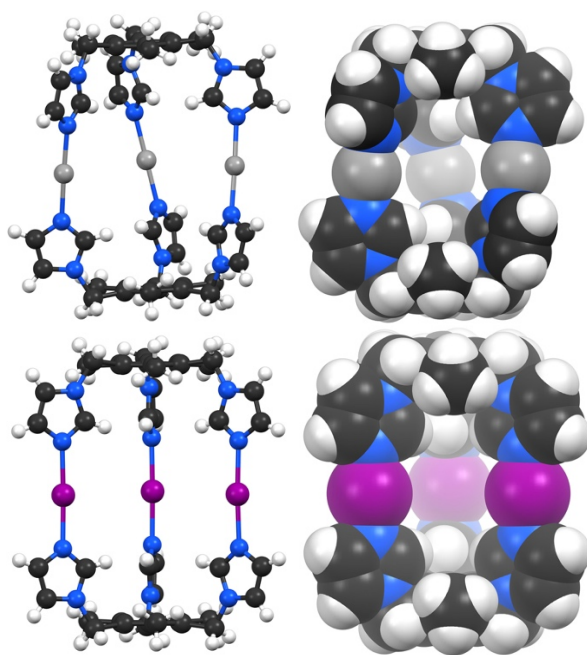


**Figure 3.** The ball-and-stick and CPK (right) presentations of the  $D_3$  symmetric helical coordination cage  $Ag_3L_2^{3+}$  (top left) and its  $C_{3h}$  symmetric analogue,  $I_3L_2^{3+}$ , assembled using  $[N\cdots I^+\cdots N]$  3c4e halogen bond (below left). The N–Ag–N and N–I–N bond lengths (Å) and angles ( $^\circ$ ): Ag–N = 2.110(5), I–N = 2.233(6); N–Ag–N = 178.2(4), N–I–N = 177.0(4). Anions and solvent molecules are omitted for clarity.

When comparing the two structurally analogous cages,  $Ag_3L_2(PF_6)_3$  and  $I_3L_2(PF_6)_3$ , it becomes apparent that they show structural similarities but also differ significantly. The coordination environment of  $Ag^+$  in  $Ag_3L_2(PF_6)_3$  has clearly shorter Ag–N bonds [2.110(5) Å] compared to the I–N bonds [2.233(6) Å] in  $I_3L_2(PF_6)_3$ , while the N–Ag–N angles are very close to linear [178.2(4) $^\circ$ ] being remarkably similar with  $I_3L_2(PF_6)_3$ . The N–Ag–N environment is known to be easily distorted away from linearity by coordinating counteranions as demonstrated, for example, by the nitrate and azide analogues of  $Ag_3L_2(PF_6)_3$ .<sup>[19,23]</sup> On the contrary, the geometry of the  $[N\cdots I^+\cdots N]$  unit is expected to be mostly undisturbed by counteranions as the contact surface of the  $I^+$  cation, perpendicular to the  $[N\cdots I^+\cdots N]$  halogen bonds, is not electrophilic but rather charge-neutral or even nucleophilic. This is attributable to the  $p_x^2p_y^2p_z^0$  valence p-orbital occupancy of the iodonium cation.<sup>[26]</sup>

The different charge distributions of the  $Ag^+$  and  $I^+$  cations is reflected also in the host-guest chemistry of the respective supramolecular  $M_3L_2^{3+}$  cages. In the solid state  $Ag_3L_2^{3+}$  clearly encapsulates one  $PF_6^-$  anion within its endohedral cavity. The  $PF_6^-$  is severely disordered over three major symmetry-related positions which were analyzed to reside at the Ag–Ag–Ag plane and being stabilized by van der Waals contacts between fluorine atoms and  $Ag^+$  ( $d(F\cdots Ag) \approx 3.0 - 3.1$  Å). This analysis is supported by an earlier study of a hydrate structure of  $Ag_3L_2(PF_6)_3$  in which the equatorial fluorine atoms of an

encapsulated (non-disordered)  $PF_6^-$  anion reside at the Ag–Ag–Ag plane within 2.8 - 3.1 Å away from the  $Ag^+$  cations.<sup>[24]</sup> In the case of  $I_3L_2(PF_6)_3$  the residual electron density suggests that one  $PF_6^-$  anion occupies the endohedral cavity and is disordered over two major positions along the  $C_3$  axis of the host, perpendicular to the I–I–I plane (see residual electron density maps of non-masked refinements of  $Ag_3L_2(PF_6)_3$  and  $I_3L_2(PF_6)_3$  in figure S5). This is reasonable when considering the cationic nature of the halonium cage which gives the impetus for the encapsulation of the anionic guest whereas the repulsive nature of the fluorine $\cdots I^+$  interaction perpendicular to the N–I–N bonds pushes the anion away from the I–I–I plane. Hence, although the anion within the cavity of  $I_3L_2(PF_6)_3$  could not be well resolved, the results suggest that the anisotropic charge distribution of the  $I^+$  cation has a directing effect in the host-guest chemistry of the respective supramolecular assemblies. This phenomenon could be exploited in tuning of the interior of a supramolecular host and thus gaining target-specificity toward e.g. charge-depleted guest species.

## Conclusions

This work presents the use of two structurally different N-donor tripodal ligands  $L_1(PF_6)_3$  and  $L_2$  in the formation of discrete cationic supramolecular halonium cages  $I_6L_4^{18+}$  and  $I_3L_2^{3+}$  from their parent metallosupramolecular cages  $Ag_6L_4^{18+}$  and  $Ag_3L_2^{3+}$ , respectively, by reaction with molecular iodine. In addition to comprehensive NMR spectroscopic and ESI-MS spectrometric evidence, the  $[N\cdots I^+\cdots N]$  halogen-bonded cages were structurally characterized for the first time at an atomic resolution by single crystal X-ray crystallography. The NMR spectroscopic results illustrated the difficulty of the cationic and sterically challenging ligand  $L_1(PF_6)_3$  to form the tetrameric metallosupramolecular cage with  $Ag^+$  cations in acetonitrile, whereas the robust  $[N\cdots Ag^+\cdots N] \rightarrow [N\cdots I^+\cdots N]$  cation exchange reaction resulted effortlessly in the desired tetrahedral  $I_6L_4^{18+}$  halonium cage. Despite the different behavior of the  $Ag^+$  and  $I^+$  cations with  $L_1(PF_6)_3$  in solution, both tetrameric  $M_6L_4$  ( $M = Ag$  or  $I$ ) cages could be obtained and characterized in the solid state by single crystal X-ray crystallography. In the case of the ligand  $L_2$ , selective formation of dimeric  $M_3L_2X_3$  cages with  $AgPF_6$  and subsequently with  $I^+$  in solution, in the gas phase and in the solid state was observed.

In conclusion, the results presented herein show that the  $[N\cdots I^+\cdots N]$  halogen bonds are very robust and reliable connectors when constructing large supramolecular assemblies with predictable structural features. The robustness of the  $[N\cdots I^+\cdots N]$  unit is highlighted by the fact that, although the native iodonium cation ( $I^+$ ) is considered to be a highly reactive species the  $[N\cdots Ag^+\cdots N] \rightarrow [N\cdots I^+\cdots N]$  cation exchange reaction does not need dry solvents during the self-assembly process or during the analyses. The crystal structures of the halonium cages clearly demonstrate the propensity of the  $[N\cdots I^+\cdots N]$  motif to systematically yield linear coordination whereas the analogous  $[N\cdots Ag^+\cdots N]$  unit is more prone to deformation. This difference would be more dramatic in the presence of coordinating anions

instead of the weakly coordinating hexafluorophosphate used in this study. The anisotropic charge density sets  $I^+$  apart from typical d-block metal cations and offers further possibilities regarding reactivity and host-guest chemistry in the context of  $[N \cdots I^+ \cdots N]$  based supramolecular systems.

## Experimental Section

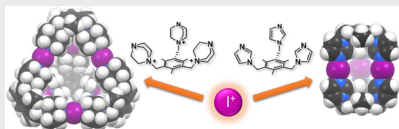
Ligands **L1**(PF<sub>6</sub>)<sub>3</sub> and **L2** were synthesized according to the reported procedures.<sup>[16,17]</sup> NMR spectra were recorded on a Bruker Avance III 500 or Avance 400 spectrometers. All signals are given as  $\delta$  values in ppm using residual solvent signals as the internal standard. ESI-MS experiments were performed on AB Sciex QSTAR Elite ESI-Q-TOF mass spectrometer equipped with an API 200 TurbolonSpray ESI source from AB Sciex (former MDS Sciex) in Concord, Ontario (Canada). Single crystal X-ray data were collected with either Agilent SuperNova, equipped with multilayer optics monochromated dual source (Cu and Mo) and Atlas detector, using Cu K $\alpha$  (1.54184 Å) radiation or Bruker-Nonius/Kappa CCD diffractometer using Mo K $\alpha$  (0.71073 Å) radiation. In the latter case, data acquisitions, reductions and absorption corrections were made using programs COLLECT<sup>[27]</sup>, DENZO-SMN<sup>[28]</sup> and SADABS<sup>[29]</sup> whereas the data collected with Agilent SuperNova was treated within the CrysAlis<sup>Pro</sup> program package<sup>[30]</sup>. The structures were solved with ShelXS<sup>[31]</sup> program and refined on  $F^2$  by full matrix least squares techniques with ShelXL<sup>[32]</sup> program in Olex<sup>2</sup> (v.1.2)<sup>[33]</sup> program package. Anisotropic displacement parameters were applied for all atoms except hydrogens which were calculated into their ideal positions using isotropic displacement parameters 1.2-1.5 times of the host atom. Olex<sup>2</sup> solvent mask routine was used to treat the residual electron density corresponding to disordered anions and solvent molecules in the crystal lattices. Details of solvent mask procedure together with crystallographic data table can be found in ESI (table S2).

## Acknowledgements

The authors kindly acknowledge the Academy of Finland (K.R.: nos. 263256, 265328, 292746; E.K.: nos. 284562 and 278743; M.L.: no. 277250). **Keywords:** halogen bond • N-donor ligand • supramolecular chemistry • X-ray crystallography • cation exchange

- [1] G. R. Desiraju, P. S. Ho, L. Kloo, A. C. Legon, R. Marquardt, P. Metrangolo, P. Politzer, G. Resnati, K. Rissanen, *Pure Appl. Chem.* **2013**, *85*, 1711–1713.
- [2] G. Cavallo, P. Metrangolo, R. Milani, T. Pilati, A. Priimagi, G. Resnati, G. Terraneo, *Chem. Rev.* **2016**, *116*, 2478–2601.
- [3] A. C. C. Carlsson, J. Gräfenstein, A. Budnjo, J. L. Laurila, J. Bergquist, A. Karim, R. Kleinmaier, U. Brath, M. Erdélyi, *J. Am. Chem. Soc.* **2012**, *134*, 5706–5715.
- [4] S. B. Hakkert, M. Erdélyi, *J. Phys. Org. Chem.* **2015**, *28*, 226–233.
- [5] A.-C. C. Carlsson, M. Uhrbom, A. Karim, U. Brath, J. Gräfenstein, M. Erdélyi, *CrystEngComm* **2013**, *15*, 3087.
- [6] M. Bedin, A. Karim, M. Reitti, A.-C. C. Carlsson, F. Topić, M. Cetina, F. Pan, V. Havel, F. Al-Ameri, V. Sindelar, K. Rissanen, J. Gräfenstein, M. Erdélyi, *Chem. Sci.* **2015**, *6*, 3746–3756.
- [7] A. C. C. Carlsson, K. Mehmeti, M. Uhrbom, A. Karim, M. Bedin, R. Puttreddy, R. Kleinmaier, A. A. Neverov, B. Nekoueshahraki, J. Gräfenstein, K. Rissanen, M. Erdélyi, *J. Am. Chem. Soc.* **2016**, *138*, 9853–9863.
- [8] a) L. Turunen, U. Warzok, R. Puttreddy, N. K. Beyeh, C. A. Schalley, K. Rissanen, *Angew. Chem. Int. Ed.* **2016**, *55*, 14033–14036. b) L. Turunen, U. Warzok, C. A. Schalley, K. Rissanen, *Chem.* submitted.
- [9] T. R. Cook, V. Vajpayee, M. H. Lee, P. J. Stang, K. W. Chi, *Acc. Chem. Res.* **2013**, *46*, 2464–2474.
- [10] K. Harris, D. Fujita, M. Fujita, *Chem. Commun.* **2013**, *49*, 6703–6712.
- [11] M. Han, D. M. Engelhard, G. H. Clever, *Chem. Soc. Rev.* **2014**, *43*, 1848–1860.
- [12] T. R. Cook, P. J. Stang, *Chem. Rev.* **2015**, *115*, 7001–7045.
- [13] A. Galan, P. Ballester, *Chem. Soc. Rev.* **2016**, *45*, 1720–1737.
- [14] M. Fujita, S. Nagao, K. Ogura, *J. Am. Chem. Soc.* **1995**, *117*, 1649–1650.
- [15] H.-K. Liu, W.-Y. Sun, D.-J. Ma, W.-X. Tang, K.-B. Yu, *Chem. Commun.* **2000**, *3*, 591–592.
- [16] P. J. Garratt, A. J. Ibbett, J. E. Ladbury, R. O'Brien, M. B. Hursthouse, K. M. A. Malik, *Tetrahedron* **1998**, *54*, 949–968.
- [17] Y. Yuan, Z. Jiang, J. Yan, G. Gao, A. S. C. Chan, R.-G. Xie, *Synth. Commun.* **2000**, *30*, 4555–4561.
- [18] H.-K. Liu, X. Tong, *Chem. Commun.* **2002**, 1316–1317.
- [19] J. Fan, H. F. Zhu, T. A. Okamura, W. Y. Sun, W. X. Tang, N. Ueyama, *Chem. Eur. J.* **2003**, *9*, 4724–4731.
- [20] J. Fan, B. Sui, T. Okamura, W.-Y. Sun, W.-X. Tang, N. Ueyama, *J. Chem. Soc. Dalton Trans.* **2002**, *3*, 3868–3873.
- [21] W.-Y. Sun, J. Fan, T. Okamura, J. Xie, K.-B. Yu, N. Ueyama, *Chem. Eur. J.* **2001**, *7*, 2557–2562.
- [22] A. Peuronen, S. Forsblom, M. Lahtinen, *Chem. Commun.* **2014**, *50*, 5469–5472.
- [23] J. Fan, W.-Y. Sun, T. Okamura, J. Xie, W.-X. Tang, N. Ueyama, *New J. Chem.* **2002**, *26*, 199–201.
- [24] H.-K. Liu, X. Huang, T. Lu, X. Wang, W.-Y. Sun, B.-S. Kang, *Dalton Trans.* **2008**, *3*, 3178–3188.
- [25] I. J. Bruno, J. C. Cole, P. R. Edgington, M. Kessler, C. F. Macrae, P. McCabe, J. Pearson, R. Taylor, C. R. Groom, I. J. Bruno, M. P. Lightfoot, S. C. Ward, *Acta Cryst.* **2016**, *72*, 389–397.
- [26] R. D. Parra, *Molecules* **2014**, *19*, 1069–1084.
- [27] R. W. W. Hooft, *Collect. Nonius BV, Delft, Netherlands* **1998**.
- [28] Z. Otwinowski, W. Minor, *Methods Enzymol.* **1997**, *276*, 307–326.
- [29] G. M. Sheldrick, *SADABS, Univ. Göttingen, Göttingen, Ger.* **2012**.
- [30] *CrysAlisPro program, version 1.171.38.43, Rigaku Oxford Diffraction, Oxford*, **2015**.
- [31] G. M. Sheldrick, *Acta Cryst.* **2007**, *64*, 112–122.
- [32] G. M. Sheldrick, *Acta Cryst.* **2015**, *71*, 3–8.
- [33] O. V. Dolomanov, L. J. Bourhis, R. J. Gildea, J. A. K. Howard, H. Puschmann, *J. Appl. Crystallogr.* **2009**, *42*, 339–341.

## FULL PAPER



Applying the robust  $[N \cdots Ag^+ \cdots N] \rightarrow [N \cdots I^+ \cdots N]$  cation exchange reaction to silver metallocages from tripodal *N*-donor halogen ligands results in the corresponding halonium cages.

Lotta Turunen Anssi Peuronen<sup>1</sup> &  
Forsblom, Elina Kalenius, Manu  
Lahtinen\* and Kari Rissanen\*

Page No. – Page No.

Title

Accepted Manuscript